

## Three-body halos: Gross properties

D. V. Fedorov,\* A. S. Jensen, and K. Riisager

*Institute of Physics and Astronomy, Aarhus University, DK-8000 Aarhus C, Denmark*

(Received 10 August 1993)

Three-body bound systems are investigated in the limit of very weak binding by use of hyperspherical harmonics. The short-range two-body potentials are assumed to be unable to bind the binary subsystems. Then the mean square radius always converges for vanishing binding except for the most spherical wave function, where all angular momenta involved are zero, which diverges logarithmically. Universal scaling properties are suggested. Any additional long-range repulsive potential, like, for example, the Coulomb potential, leads to finite radial moments even for vanishing binding. Spatially extended charged halos are only possible for very low charges. The spatial extension of three-body systems is in the asymptotic region more confined than for corresponding two-body systems, where the divergences are stronger and more abundant. Numerical examples and transitions to the asymptotic region are shown for square well and Gaussian two-body potentials. The results are applied to several drip-line nuclei.

PACS number(s): 21.45.+v, 21.60.Gx

### I. INTRODUCTION

Halo nuclei [1], i.e. nuclear systems with an unusually large spatial extension, are by now well established on the neutron drip line [2,3]. The principle behind the halo formation is simple and directly related to the weak binding of the last one or two neutrons. A general survey of static properties and occurrences of two-body halos recently gave additional insight into these simple systems [4]. A recent comparison between one- and two-neutron halo systems also led to surprising conclusions [5]. Many other interesting and more complicated structures may also be anticipated [6-8]

Of particular interest are three-body bound systems where furthermore all two-particle subsystems are unbound, the so-called Borromean nuclei [9]. They are presumably quite common along the neutron drip line. The three-body structure with an inert core and two (inert) halo particles is, at least to a large extent, realized in several light nuclei [9]. We shall make the overall assumption that the core and halo degrees of freedom are completely decoupled. Such studies thus become rather meaningless, when they are extended to accuracies where the core degrees of freedom begin to contribute.

The purpose of the present paper is to investigate the asymptotic behavior of weakly bound three-body systems in general, to establish common features and in analogy to Ref. [4] also characterize the large distance properties. We shall make the incorrect assumption that the constituent particles are spinless which implies that there then is also no spin-orbit interaction. These simplifications are not basic limitations and improvements are ob-

viously possible. However, this may serve to illustrate our aim, which is to extract essential and general properties for the three-body system. Our model systems are at best only approximations of real systems in nature and also for this reason one should not push the accuracy level too far. On the other hand, clean mathematical reference models are often very useful and we shall try to extract the gross properties of physical relevance.

This paper is intended to be the first in a series of papers discussing various aspects of three-body halos. After the Introduction we give first in Sec. II a theoretical discussion of the behavior of Borromean nuclei in the asymptotic weak-binding limit. A few necessary mathematical definitions and details are collected in the Appendix. In Sec. III we illustrate the behavior by numerical examples where square wells and Gaussian potentials are used. In Sec. IV we give criteria for the appearance of halo nuclei and list a number of nuclear halo candidates. Finally Sec. V gives the conclusions.

### II. THEORY

We shall consider a three-body system consisting of an inert core and two halo particles. They are assumed to be spinless and to interact via weak two-body central potentials, which have no bound binary subsystem, but where the total three-body system can exist in a bound state. The spin-orbit interactions are in other words not included explicitly, but their diagonal parts are accounted for by adjustments of the strengths of the central potentials. We shall focus on states lying just below the three-body threshold. We note for completeness that the Efimov effect [6], a pathology in three-body systems that also involves loosely bound states, occurs close to a two-body threshold, i.e., in a region where the present treatment becomes invalid.

Several methods have already been used to describe

---

\*On leave from the Kurchatov Institute, 123182 Moscow, Russia.

halo nuclei. Among them are the variational approach [10], the cluster-orbital shell model [11], the two-particle Green's function method [12], the variational shell model [13], the coordinate space Faddeev approach, and the hyperspherical harmonics method [9]. We shall here employ the latter that allows a rather transparent formulation of the problem.

### A. The hyperspherical expansion

The total wave function  $\Psi$  of a three-body system (excluding the center-of-mass degrees of freedom) may be expanded in terms of the hyperspherical h [6–8]armonics  $\mathbf{Y}_K$  as [14–16]

$$\Psi(\rho, \Omega) = \frac{1}{\rho^{5/2}} \sum_{\mathcal{K}} f_{\mathcal{K}}(\rho) \mathbf{Y}_{\mathcal{K}}(\Omega), \quad (1)$$

where  $\rho$  is a generalized radial coordinate (the sum of squares of Jacobi coordinates) and the remaining five degrees of freedom have been transformed into angular variables in  $\Omega$  (the direction of the two Jacobi coordinates and the inverse tangent of the ratio of their lengths). The coordinate systems are shown in Fig. 1. This expansion is complete and is analogous to that of a two-body wave function in terms of spherical harmonics, the spherical quantum numbers  $l, m$  being replaced by a set  $\mathcal{K}$  of corresponding so-called hyperspherical quantum numbers. The functions  $\mathbf{Y}_{\mathcal{K}}$  are eigenfunctions of an angular operator  $\hat{K}^2(\Omega)$  with eigenvalues  $K(K+4)$  where the quantum number  $K$  (usually called hypermoment) is a non-negative integer, even or odd depending on the parity of the system. The value of  $K$  defines the effective centrifugal barrier.

The Hamiltonian of the system, where the center-of-mass kinetic energy is subtracted, is given by

$$H = \sum_{i=1}^3 \frac{p_i^2}{2m_i} - \frac{P^2}{2M} + \sum_{i>j=1}^3 V_{ij}(r_{ij}), \quad (2)$$

where  $m_i$ ,  $\mathbf{r}_i$ , and  $\mathbf{p}_i$  are mass, coordinate, and momentum of the  $i$ th particle,  $V_{ij}$  are the two-body potentials,  $P$  and  $M$  are the total momentum and the total mass,

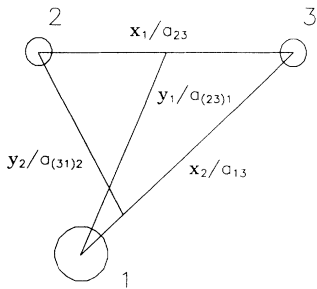


FIG. 1. The Jacobi coordinates used to describe the three-body system, see also the Appendix. Note that for a heavy core (particle 1)  $\mathbf{x}_2$  and  $\mathbf{y}_2$  become the relative coordinates of the light particles (2 and 3) against the core.

and  $\mathbf{r}_{ij} = \mathbf{r}_i - \mathbf{r}_j$ .

From the Schrödinger equation one obtains [16] the following set of coupled differential equations for the radial functions  $f_{\mathcal{K}}$ :

$$\begin{aligned} & \left( -\frac{d^2}{d\rho^2} + \frac{(K+3/2)(K+5/2)}{\rho^2} \right. \\ & \left. + \frac{2m}{\hbar^2} W_{\mathcal{K}\mathcal{K}}(\rho) - \frac{2m}{\hbar^2} E \right) f_{\mathcal{K}}(\rho) \\ & = -\frac{2m}{\hbar^2} \sum_{\mathcal{K}' \neq \mathcal{K}} W_{\mathcal{K}\mathcal{K}'}(\rho) f_{\mathcal{K}'}(\rho), \end{aligned} \quad (3)$$

where  $E$  is the energy and  $m$  is the nucleon mass chosen as a normalizing constant when defining the Jacobi variables (see the Appendix). The effective potentials  $W$  are given in terms of the two-body potentials  $V_{ij}$  by

$$W_{\mathcal{K}\mathcal{K}'}(\rho) = \int d\Omega \mathbf{Y}_{\mathcal{K}}(\Omega) \mathbf{Y}_{\mathcal{K}'}(\Omega) \sum_{i>j=1}^3 V_{ij}(r_{ij}), \quad (4)$$

where  $d\Omega = \cos^2 \alpha \sin^2 \alpha d\alpha d\Omega_x d\Omega_y$  is the angular volume element for the directions of the two Jacobi coordinates and for  $\alpha$ , which is in the interval  $[0, \pi/2]$ . In the lowest-order approximation where off-diagonal terms are neglected, the right-hand side of Eq. (3) is put equal to zero and the resulting equation is very similar to that of a two-body system. The centrifugal barrier, however, does not vanish even for the lowest value of  $K = 0$ . This fact is directly related to the larger dimension of the kinetic energy operator [5]. The effective potential in the resulting one-dimensional radial Equation (3) is simply the matrix element of the two-body potentials between the hyperspherical harmonics, see Eq. (4).

We assume in this paper that there are no bound states in any of the two-body subsystems. In this case the asymptotic form [17] of the wave function is  $\rho^{-5/2} \exp(-\rho \sqrt{-2mE/\hbar^2})$  and the expansion of the wave function in terms of hyperspherical harmonics converges rather fast. The physical reason for the rapid convergence of the hyperharmonic expansion of the wave function is that the height of the centrifugal barrier  $(K+3/2)(K+5/2)/\rho^2$  increases rapidly with  $K$ . This substantially reduces the contributions from the higher  $K$  values in the total wave function.

The Pauli principle requires that the solutions are orthogonal to the occupied core states. The easiest way to achieve this approximately is to exclude the lowest lying states occupied by core nucleons and consider the first unoccupied state. An alternative way is to introduce a repulsive neutron-core potential in the corresponding states. With the above asymptotics the lowest non-Pauli forbidden  $K$  value in the expansion usually gives a good approximation to the total wave function of the three-body system; see, e.g., [18,19]. In any case we shall maintain the expansion in Eq. (1) and investigate the properties of the radial functions for all  $K$ . It turns out that in the asymptotic low binding limit, the largest contributions to the radial moments come from the terms

of lowest  $K$ , again demonstrating the convenience of this method of expansion.

### B. Matrix elements of a short-range potential

The decisive quantity in the equations of motion, Eq. (3), is the effective potential  $W$  arising from the various two-body potentials. We look first at the contribution to  $W$  from a short-range two-body central potential  $V(r)$ . In the present context we shall define short range as a potential that decreases faster than any power of the radial variable. This is a more restrictive definition than used in Ref. [4]. The matrix element is computed by a change of variables to  $\rho$  and  $\Omega$ . The distance  $r$  between the two particles becomes  $r = (\rho/a) \cos \alpha$ , where  $a$  is the square root of the reduced mass in units of the nucleon mass corresponding to the two-body system involved. The contribution to  $W$  from a two-body potential  $V$  is then given by

$$\int d\Omega \mathbf{Y}_{\mathcal{K}}(\Omega) \mathbf{Y}_{\mathcal{K}'}(\Omega) V\left(\frac{1}{a} \rho \cos \alpha\right). \quad (5)$$

In the large-distance limit of  $\rho \gg r_0$ , where  $r_0$  is the radius beyond which the potential can be neglected, the integrand in Eq. (5) vanishes unless  $\pi/2 - \epsilon < \alpha < \pi/2$ , where  $\epsilon = \arcsin(ar_0/\rho) \approx ar_0/\rho$  is a small quantity. The Jacobi polynomials in the hyperharmonics are then approximately constant and the angles  $d\Omega_x$  and  $d\Omega_y$  are then easily integrated out. Apart from the potential strength parameters and other normalization constants, one obtains therefore the large-distance behavior of the effective potentials as [20]

$$\begin{aligned} W_{\mathcal{K}\mathcal{K}'}(\rho) &\propto \delta_{l_x l'_x} \delta_{l_y l'_y} \delta_{LL'} \int_{\pi/2-\epsilon}^{\pi/2} d\alpha (\cos \alpha)^{2l_x+2} \\ &\propto \delta_{l_x l'_x} \delta_{l_y l'_y} \delta_{LL'} \left(\frac{ar_0}{\rho}\right)^{2l_x+3}. \end{aligned} \quad (6)$$

Only diagonal terms in the angular momentum quantum numbers appear, whereas the long-distance behavior of the potentials is independent of the radial quantum numbers  $K$  and  $K'$ . Thus, a short-range two-body potential gives an effective  $\rho$ -dependent potential that has the long-distance asymptotic form  $\rho^{-n}$ , where  $n \geq 3$ . This is faster than the always present centrifugal barrier and therefore unimportant for large distances.

### C. Weak-binding limit for short-range potentials

The radial potentials arising from the short-range two-body potentials are all decreasing faster at large distances than the generalized centrifugal barrier term. Since the radial wave functions,  $f_{\mathcal{K}}$ , all decrease exponentially with  $\rho$ , provided no binary subsystem is bound [17], we can conclude that the equations of motion, Eq. (3), decouple in the asymptotic large-distance limit. The radial wave functions in this region, where the matrix elements of the

short-range potentials are negligible, are solutions to the following simple equation:

$$-\frac{d^2}{d\rho^2} f_{\mathcal{K}} + \frac{(K+3/2)(K+5/2)}{\rho^2} f_{\mathcal{K}} + \kappa^2 f_{\mathcal{K}} = 0, \quad (7)$$

where  $\kappa^2 = -2mE/\hbar^2$ . This equation is valid for  $\rho > \rho_L$ , where  $\rho_L$  is the radius beyond which the potentials  $W$  in Eq. (3) can be neglected compared to the centrifugal barrier term. The corresponding solution is a modified Bessel function with asymptotic forms  $e^{-z}$  and  $z^{-K-3/2}$ , respectively, for large and small values of  $z = \kappa\rho$ . The potential at smaller distances is not specified at the moment and we shall only assume that the energy is a smooth function of the parameters of the potentials  $V_{ij}$  and that the wave functions are well behaved for  $\rho < \rho_L$ , in particular that  $f_{\mathcal{K}}(\rho_L)$  are finite.

The key quantities describing the size of the system are the moments of  $\rho$  which may be divided into contributions from the inner ( $\rho < \rho_L$ ) and outer ( $\rho > \rho_L$ ) region:

$$\langle \rho^n \rangle = \sum_K [I_n(K) + O_n(K)]. \quad (8)$$

The inner parts  $I_n$  of these integrals are finite for all bound systems. The outer parts

$$O_n = \int_{\rho_L}^{\infty} f_{\mathcal{K}}^2(\rho) \rho^n d\rho \quad (9)$$

may be evaluated in the limit of vanishing binding energy. In complete analogy to Ref. [4] (substituting  $K+3/2$  for  $l$ ), we obtain the following scaling behavior for small  $\kappa$ :

$$\begin{aligned} O_n &\propto \kappa^{2K+2-n} \left( \text{const} + \int_{\kappa\rho_L}^{\delta} z^{-2K-3+n} dz \right) \\ &\propto \begin{cases} (\rho_L \kappa)^{-n+2K+2}, & n > 2K+2, \\ \ln(\rho_L \kappa), & n = 2K+2, \\ \text{const}, & n < 2K+2, \end{cases} \end{aligned} \quad (10)$$

where  $\delta$  is a nonvanishing small number.

We can now extract a few important conclusions. Normalization of the wave function involves  $O_0$  which always is finite even when the energy goes to zero. The rms (root mean square) radius involves  $O_2$  and diverges logarithmically for  $K=0$  and converges for  $K>0$ . In general, for any given  $n$  the lowest  $K$  in the expansion in Eq. (1) leads to the fastest divergence provided the moment is divergent at all, i.e., if  $n \geq 2K_{\min} + 2$  where  $K_{\min}$  is the lowest possible  $K$  value. When  $K_{\min}$  also is the dominating component in the wave function, the scaling properties at low binding are those of  $O_n(K=K_{\min})$ . When the main component has a value of  $K$  larger than  $K_{\min}$ , the limiting behavior will at first be determined by the main component. Ultimately the lowest  $K$  value will dominate, unless of course its weight simultaneously approaches zero.

It is rather easy to estimate when a smaller component from a lower  $K$  value will catch up with the dominating term. The difference in  $K$  is at least two, as the terms

should have the same parity. When both terms diverge one sees from Eq. (10), upper line, that the difference in weight can be compensated by the difference of four powers of  $\kappa\rho_L$ . For an admixture of the lower  $K$  value of a few percent this corresponds to a binding energy of about 200 keV. This result is unchanged when the main term leads to a logarithmic divergence ( $n = 2K + 2$ ), which is very slow in the present context. Finally, when the admixture diverges logarithmically the leading term is convergent, and the energy of equal contribution will be on the eV scale.

We shall close this section by emphasizing that the three-body system behaves quite different from the two-body system in the low-binding limit. The probability for finding the “halo” inside the range of the “core” potential is finite for all relative angular momenta even for vanishing binding energy ( $O_0$  remains constant). The asymptotic value of the second radial moment behaves like

$$\langle \rho^2 \rangle \rightarrow \begin{cases} \ln(\kappa\rho_L), & K = 0, \\ \text{const}, & K \neq 0, \end{cases} \quad (11)$$

where  $K$  is the dominating term in the wave function. For  $K = 0$  no admixture of lower values can occur and for a nonzero  $K$  value, the worst divergence from an admixture would be logarithmic and as such not noticeable for energies above the eV region for admixtures on the 5% level. The results expressed in Eq. (11) are therefore in most cases accurate although not completely stringent.

The moments of the effective radial coordinate  $\rho$  are the basic quantities from which we may compute all other radial moments. In particular the moments related to the distances  $x$  and  $y$  between the three particles are interesting. In the only case of diverging mean square radius,  $K = 0$ , all angular momenta are zero and the wave function is  $\Psi(\rho, \Omega) = \pi^{-3/2} f_0(\rho) \rho^{-5/2}$ . We therefore have  $\langle x^2 \rangle = \langle y^2 \rangle = \langle \rho^2 \rangle / 2$  from which we get the physical mean square values by multiplying with appropriate ratios of reduced masses. For two neutrons around a core with mass number  $A_c$ , we obtain from the Appendix  $\langle r_{nn}^2 \rangle = \langle \rho^2 \rangle$  and  $\langle r_{(nn)c}^2 \rangle = (1 + 2/A_c) \langle \rho^2 \rangle / 4$ , where  $r_{nn}$  and  $r_{(nn)c}$ , respectively, are the distance between the neutrons and their center of mass distance from the core.

#### D. Weak-binding limit for $r^{-\nu}$ potentials

We shall now consider the case where the two-body potential of longest range has the form  $V(r) = S/r^\nu$  where  $S$  is the strength of the potential. We shall only consider repulsive potentials ( $S > 0$ ) which fall off slower than  $r^{-3}$  ( $\nu < 3$ ). Otherwise the core will become too repulsive and the integrals in the matrix elements  $W_{\mathcal{K}\mathcal{K}'}$  will diverge. Clearly the large-distance behavior of these effective potentials is the same as for the original two-body potential. They can be neglected compared to the centrifugal barrier at large  $\rho$  for  $2 < \nu < 3$ , in which case all the above results derived for short-range potentials are valid.

If  $\nu = 2$ , we must keep the diagonal contribution from  $W$  in Eq. (7). This amounts to a renormalized larger value of  $K$  which in turn should be used in the scaling behavior of  $O_n$  in Eqs. (10) and (11). Thus also the second radial moment of  $K = 0$  is convergent.

When  $0 < \nu < 2$ , we are not mathematically allowed to neglect the nondiagonal coupling terms in the equations of motion. In other words, the equations do not necessarily decouple at large distances as for short-range potentials. On the other hand, several computations, where the Coulomb potential is included and  $K$  mixture is allowed, still led to solutions, where one  $K$  value dominates the wave function; see refs. [16,18]. Furthermore, the repulsive barrier clearly squeezes a bound system towards smaller radii, which will diminish the coupling at large distances. We shall therefore assume that the off-diagonal matrix elements can be neglected. Physically this seems to be a very reasonable assumption in our case, although a different large-distance behavior of the components of the wave function mathematically cannot be excluded.

The uncoupled one-dimensional radial Schrödinger equation is now given by

$$-\frac{d^2}{d\rho^2} f_\kappa + \frac{(K + 3/2)(K + 5/2)}{\rho^2} f_\kappa + \frac{\lambda}{\rho^\nu} f_\kappa + \kappa^2 f_\kappa = 0, \quad (12)$$

where  $\lambda$  is determined from Eq. (4). As we have assumed a repulsive potential and therefore a positive  $\lambda$  value, we can now introduce the dimensionless variable  $z = \lambda^{1/(2-\nu)} \rho$  and obtain

$$O_n = \lambda^{-\frac{n-1}{2-\nu}} \int_{z_L}^{\infty} w^2(z) z^n dz, \quad (13)$$

where  $z_L = \lambda^{1/(2-\nu)} \rho_L$  and  $w(z) = f_\kappa(z \lambda^{\nu/2})$ .

The lower limit of the integral in  $O_n$  is finite, since both  $\lambda$  and  $\rho_L$  are finite and independent of energy. The integrand consequently remains finite at the lower limit. The large-distance asymptotic behavior may be determined from the asymptotic ( $z$  large) equation for vanishing energy,  $w'' = w/z^\nu$ , which has the asymptotic large-distance solution

$$w \rightarrow z^{\nu/4} \exp\left(-\frac{2}{2-\nu} z^{\frac{2-\nu}{2}}\right). \quad (14)$$

Thus, the integral in  $O_n$  also receives finite contribution from large distances and the conclusion is that any repulsive two-body potential of the kind  $r^{-\nu}$ ,  $0 < \nu < 2$ , leads to diagonal solutions where all radial moments remain finite.

A particularly important example is the Coulomb potential corresponding to  $\nu = 1$ . This case applies in other words to charged particles in the halo of the three-body system. The diagonal strength parameter  $\lambda = (2m/\hbar^2) \sum_i Z_j Z_k e^2 a_i / 16 / (3\pi)$  is obtained from Eq. (4) for  $K = 0$ . The asymptotic form of the wave function for vanishing binding energy is now  $(\lambda\rho)^{1/4} \exp(-2\sqrt{\lambda\rho})$ . This is a slower falloff than for the familiar exponential

obtained for neutral systems at a finite binding energy (or equivalently for a constant potential barrier extending to infinity), but the falloff is not slow enough to cause divergences. As for the general case above, we conclude that all radial moments are finite. The binding energy is either negative, and the system unstable, or positive and the system remains finite no matter how close the binding energy approaches zero.

### III. NUMERICAL RESULTS

To illustrate the actual behavior of three-body systems, we must specify the two-body potentials. We shall in this section consider two nucleons outside a heavier core. The nucleon-nucleon potential is kept fixed in all calculations, whereas the nucleon-core potential is varied to change the binding energy of the total system.

The nucleon-nucleon potential is chosen to reproduce free low-energy scattering data for identical nucleons. This can be achieved if the observed singlet  $s$ -wave scattering length and the effective range both are reproduced by a simple potential. Other properties are expected to be rather insignificant for the present purpose of studying weakly bound systems. We use a square well potential [ $S_{nn}\Theta(r < R_{nn})$ ] with the strength  $S_{nn} = -13.4$  MeV and a radius parameter  $R_{nn} = 2.65$  fm from Ref. [21]. For comparison we tried a Gaussian potential [ $S_{nn}\exp(-r^2/b_{nn}^2)$ ] with strength  $S_{nn} = -31$  MeV and range parameter  $b_{nn} = 1.8$  fm from Ref. [10]. In addition, we also used the Gogny-Pires-de Toureil (GPT) potential consisting of three Gaussians [22]. These potentials, reproducing the low-energy scattering neutron-neutron data, will be used throughout also for neutron-proton halos.

#### A. Scaling properties

It is well known that the spherical two-body problem with a square well potential has scaling properties between size and energy. This is easily obtained by multiplying all energies by  $R_0^2$  and dividing all lengths by  $R_0$ , where  $R_0$  is the potential radius. For a Gaussian potential a similar scaling holds with  $R_0$  substituted by the range parameter  $b$ . All sizes of the potential and in fact also potentials of different shapes then results in one universal curve for each angular momentum; see also Ref. [5]. This is clearly a very simplifying feature which allows an easy overview.

The three-body problem is different, since our effective radial equation receives contributions from three short-range potentials and possibly also from Coulomb interactions. However, scaling may still be approximately valid, provided a single effective  $\rho$  potential can be used to reproduce the energy and mean square radius of the system. If we only consider the short-range potentials, it is reasonable to expect that the radius  $\rho_0$  of this effective potential must be an average over the individual two-body radii  $R_{ij}$ . An attempt of parametrization for square well potentials could then be

$$\rho_0^2 = \frac{\sum_{i>j=1}^3 (a_{ij}R_{ij})^2 (a_{ij}R_{ij})^2 V_{ij}}{\sum_{i>j=1}^3 (a_{ij}R_{ij})^2 V_{ij}}, \quad (15)$$

where  $V_{ij}$  are the potential depths.

This form turns out to work well in practice, although it is based only on the following heuristic arguments. All radii should enter with the square root of the corresponding reduced mass  $\mu = a^2$ , since this combination enters the effective radial Schrödinger equation. The weights in the average are conjectured to be given by the quantities  $(a_{ij}R_{ij})^2 V_{ij}$  which determine the two-body scaling. The average is taken over the radii squared (other combinations were tried, but were not as successful). Various limits of Eq. (15) are now reasonable. When all  $aR$  are equal or only one  $R$  is nonzero, the radius  $\rho_0$  reduces to the corresponding  $aR$ . We may expect that  $\rho_0$  will depend weakly on  $l_x$  through the shape of the outer part of the radial potential, see Eq. (6). We do not attempt to include this effect at the present level of accuracy, where we furthermore mainly want to consider low values of  $l_x$ .

In an application, where even the lowest lying levels of all two-body systems only are slightly unbound, we have that  $(aR)^2 V$  for a given angular momentum approximately is a constant independent of the individual two-body channel. The change in  $V$  needed for varying the binding energy is rather small and can therefore be neglected at the present level of accuracy. For ground-state  $s$  waves in all channels Eq. (15) now reduces to

$$\rho_0^2 = \frac{1}{3} \sum_{i>j=1}^3 (a_{ij}R_{ij})^2, \quad (16)$$

which in the important case of two neutrons outside a heavy core further simplifies to

$$\rho_0^2 = s_c \mu_{cn} R_{cn}^2 + s_n \mu_{nn} R_{nn}^2, \quad (17)$$

where  $R_{cn}$ ,  $R_{nn}$  and  $\mu_{cn}$ ,  $\mu_{nn}$  are the related radii and reduced masses in units of  $m$  for the subsystems and  $s_c = 2s_n = 2/3$ .

When one of the potentials has a weakly unbound  $p$  state, the strength of the potential is roughly four times as large as for the lowest  $s$  state. (This is seen from an infinite square well, where the energies are found from the zero points of the Bessel functions.) Since a state of  $K = 1$  for two nucleons outside a heavy core on average essentially corresponds to one of the nucleons in a  $p$  state and the other nucleon in an  $s$  state, the value of  $\rho_0$  is still given by Eq. (17) with  $s_c = 5s_n = 5/6$ . When the two nucleons instead are in a state of  $K = 2$  roughly corresponding to both nucleons in  $p$  states, we obtain in complete analogy again Eq. (17) with  $s_c = 8s_n = 8/9$ .

For Gaussian potentials we can most easily find the appropriate scaling rule by relating to square well potentials. The energy of a two-body system interacting through a square well potential is determined by the product of depth and radius squared. A tempting and reasonable generalization of this quantity to other spherical potentials is  $\int V r dr$ , which then should be independent of the potential for a given energy. The range pa-

parameter in a given potential  $V$  can now be related to the radius of a square well by

$$\frac{\int V r^3 dr}{\int V r dr} = \frac{\int V_{\text{sq}} r^3 dr}{\int V_{\text{sq}} r dr} = \frac{R_{\text{sq}}^2}{2}, \quad (18)$$

where we again use the second radial moment, since we only attempt to reproduce mean square radii. For a Gaussian potential with range parameter  $b$  this gives  $R_{\text{sq}} = b\sqrt{2}$ . For a Woods-Saxon potential,  $\{1 + \exp[(r - R)/a]\}^{-1}$ , it gives approximately  $R_{\text{sq}} = R\sqrt{1 + 5/3(\pi a/R)^2}$ . This relation enables us to derive the square well equivalent  $\rho_0$  to be used in the scaling of other potentials.

These prescriptions provide a rather general way of comparing the results (mean square radii and energies) for different potentials with each other as well as with measured values. Other examples may also be worked out if needed, e.g., corresponding to the first excited  $K = 0$  state where excited two-body  $s$  states contribute.

The scaling parameter  $\rho_0$  in Eq. (17) is a sum of two terms, where the neutron-core term is larger than the neutron-neutron term by roughly a factor of  $4A_c^{2/3}$ , where  $A_c$  is the mass number of the core. This factor arises by combining the weight factor 2, the reduced masses, and the ordinary estimate of nuclear radii. The scaling parameter is consequently dominated by the neutron-core interaction and rather insensitive to the actual choice of the neutron-neutron interaction.

## B. Two neutrons in the halo

We must here specify the neutron-core potential and use a square well [ $S_{cn}\Theta(r < R_{cn})$ ], a Gaussian [ $S_{cn}\exp(-r^2/b_{cn}^2)$ ], or a Woods-Saxon potential ( $S_{cn}\{1 + \exp[(r - R)/a]\}^{-1}$ ). The radius and range parameters are fixed to the values  $R_{cn} = 1, 3, 5, 7$  fm,  $b_{cn} = 2.55$  fm [10,19],  $R = 3.02$  fm, and  $a = 0.75$  fm [9], whereas the strength parameters are left as free parameters to allow for variation of the binding energy of the total system.

We illustrate first in Fig. 2 the scaling as well as the asymptotic behavior for the lowest three  $K$  values. The lines correspond to calculations with the square well potential where only a single  $K$  value is included. As the binding energy decreases, we observe that the mean square radius converges towards finite values for  $K = 1, 2$  and diverges logarithmically for  $K = 0$ . The centrifugal barrier is seen to confine the system rather strongly in perfect agreement with the general discussion in Sec. II; see, for example, Eq. (11). The limiting behavior is, like in the two-body case, essentially reached at around 1 MeV fm<sup>2</sup>. However, the asymptotic three-body system is more confined due to the larger effective centrifugal barrier. The behavior in the two cases is rather analogous, if the translation  $l = K + 3/2$  is used.

The scaling behavior suggested in Eq. (17) is followed remarkably well. Even the results for a neutron-core radius of 7 fm (not shown) can hardly be distinguished from

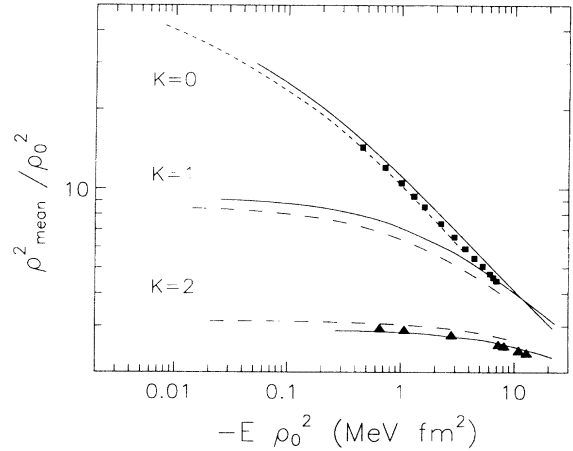


FIG. 2. The mean square radius as function of binding energy for  $K = 0, 1, 2$  for two neutrons outside a core of nine nucleons. The curves are calculated with the square well potentials using one  $K$  value only. Short-dashed, long-dashed, and full curves are for 1 fm, 3 fm, and 5 fm radii of the neutron-core potential, respectively. All are obtained with a neutron-neutron square well potential of  $S_{nn} = -13.4$  MeV and  $R_{nn} = 2.65$  fm, see Ref. [21]. The solid squares and solid triangles are for the GPT potential from Ref. [22] and a neutron-core potential specified in the text. Even though several  $K$  values were allowed the main components had  $K = 0$  and  $K = 2$ , respectively. The depth of the neutron-core potential is varied along the curves. The scaling parameter  $\rho_0$  is taken from Eqs. (17) and (18).

the other two curves with  $K = 0$ . The relative weights of the radii are about right, since the variation displayed in Fig. 2 covers the range from small to large neutron-core radii compared to the neutron-neutron radius.

The solid points in Fig. 2 are the results using several  $K$  values and Gaussian potentials (for  $K = 0$ ) or Woods-Saxon potentials (for  $K = 2$ ). For  $K = 0$  the strength  $S_{cn}$  is about  $-10$  MeV for all partial waves, for  $K = 2$  we used a repulsive  $s$ -wave potential ( $S_{cn} = 25$  MeV) and an attractive  $p$ -wave potential ( $S_{cn} \approx -22$  MeV). This latter choice makes the  $(K, L, l_x, l_y) = (2, 0, 0, 0)$  component of the wave function dominant. The value of  $\rho_0$  is obtained by use of a neutron-neutron radius of  $b = 1.8$  fm from Ref. [10] although the actual numbers were computed with a more complicated potential [22]. This is permissible as seen in Fig. 2 and as argued above. Furthermore, the calculations allow mixing of  $K$  values which means that many states of even  $K$  are mixed, but each state is still dominated by one contribution. The same energy is then found by a slightly more shallow potential, but as seen in the figure, the shape of the curves still remain unchanged. All these features underline the power of the scaling procedure, where apparently only gross features of the potential are important. Even a square well can therefore be used to obtain quantitative results with an accuracy of about 10% for pronounced halos.

The  $K$  dependence of the relative extensions of the various states may be seen in Fig. 3, where we, for a given small energy, show the probability as function of  $\rho$  for the

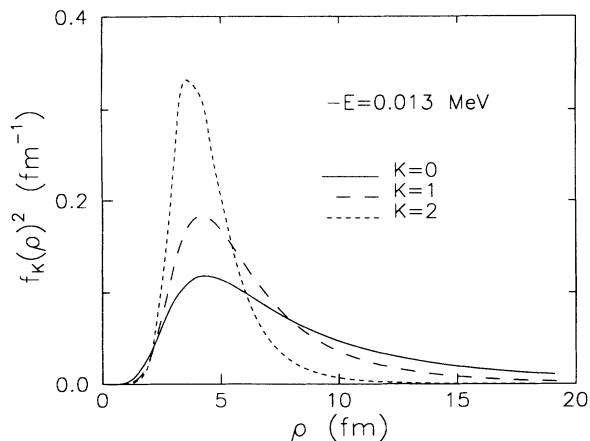


FIG. 3. The absolute square of the wave function  $f_K$  as function of  $\rho$  for the square well potentials of Fig. 2 for three  $K$  values. The binding energy is 0.013 MeV and the radius of the neutron-core potential is 3 fm.

three lowest  $K$  values. The volume element is in other words included and the integral of the plotted function is unity. The strong suppression of the tail is clearly seen as  $K$  increases, although even the  $K = 2$  state has a substantial fraction of the probability at distances outside 5 fm. The  $K = 0$  tail is significant between 10 and 15 fm corresponding to 3–5 times the radii of the square well potentials.

The energy dependence of the wave function for  $K = 0$  is shown in Fig. 4. The probability in the tail is increased substantially when the binding energy decreases from 1 MeV to 100 keV, whereas the increase is much slower when even lower binding energies are considered.

### C. Charged nucleons in the halo

When the core is charged and the halo contains protons, we must include both short-range attractions and

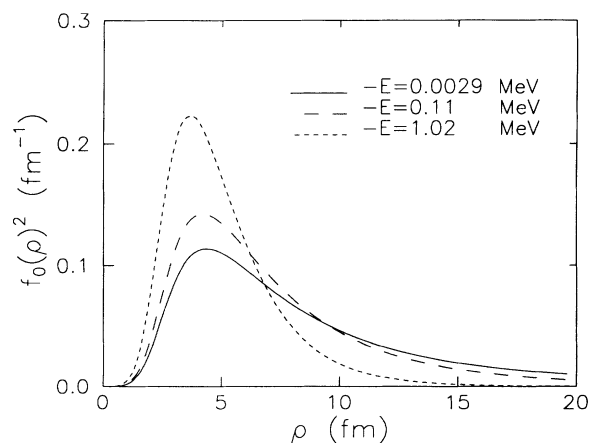


FIG. 4. The absolute square of the wave function  $f_0$  as function of  $\rho$  for the square well potentials of Fig. 2 for three binding energies. The radius of the neutron-core potential is 3 fm.

the long-range Coulomb repulsion. The potential between halo particles must be similar to the neutron-neutron potential and not deuteronlike. Otherwise a bound subsystem would appear and the present treatment would be meaningless. Here we do not treat the case of a deuteronlike structure surrounding a core even though it might give a lower energy, but concentrate instead on the isospin 1 relative halo state. Such a state could appear, for example, at high excitation energy as an isobaric analogue state of a two-neutron halo nucleus. The neutron-core and the proton-core short-range potentials are assumed to have the same range. For the following numerical calculations only the sum of the two strengths is important.

The asymptotic behavior of the mean square radius as function of energy is shown in Fig. 5 for zero, one, and two charges in the halo. The two-neutron case of Fig. 2 is included for comparison and we observe clearly the convergence at low binding energy as soon as the Coulomb potential is present. One proton in the halo still leaves room for a significant increase of size by decreasing the energy, whereas already two charges confine the system to a size almost independent of energy. Even larger charges would of course magnify this trend.

The scaling applied in Fig. 2 is used completely unchanged in Fig. 5. Since the Coulomb potential is not taken into account in the scaling rule, it is not surprising that larger deviations occur for charged particles. We notice that the (charge independent) scaling is better at larger than at smaller binding energies in accordance with the reduced influence of the Coulomb potential on strongly bound systems. The tail of the wave function decreases exponentially for strong binding, where the short-range potential itself is keeping the system confined before it is large enough to be influenced by the Coulomb potential. The opposite behavior is seen at smaller energies, where the short-range potential allows for an extended system, which then instead is squeezed by the re-

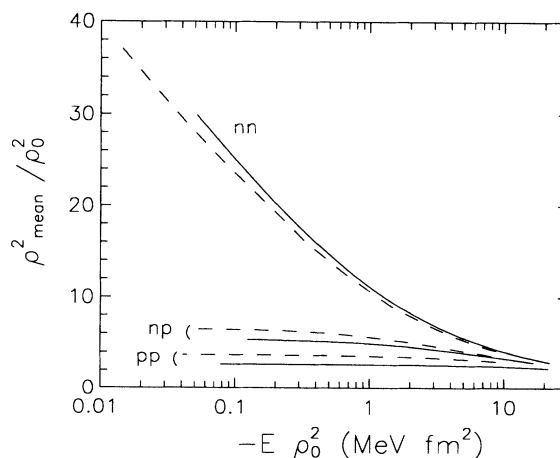


FIG. 5. The same as Fig. 2 for  $K = 0$  for two neutrons, two protons, and one neutron and one proton in the halo outside a Li core. The scaling applied is as in Fig. 2, although the Coulomb interaction is present.

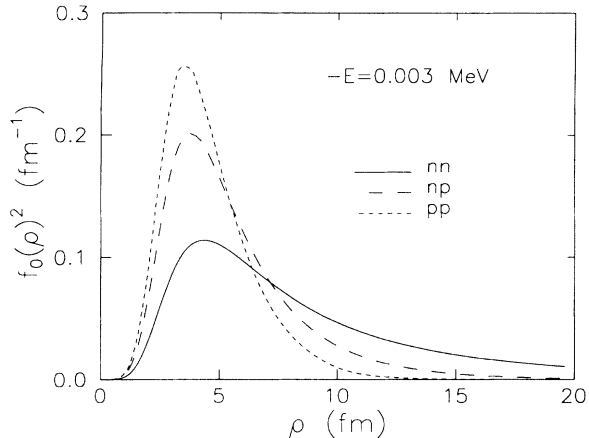


FIG. 6. The absolute square of the wave function  $f_0$  as function of  $\rho$  for the square well potentials of Fig. 2 for an energy of 3 keV for two neutrons, two protons, and one neutron and one proton in the halo outside a Li core. The radius of the neutron-core potential is 3 fm.

pulsive Coulomb potential. It is simply a question about which asymptotic behavior is the physically relevant one,  $\exp(-\kappa\rho)$  or  $\exp(-2\sqrt{\lambda\rho})$ . Mathematically it is of course the former (the latter only applies as long as the binding energy is small compared to the Coulomb potential), but if the wave function is sufficiently confined, the large distances are weakly populated and the behavior at intermediate distances is most important.

The wave functions corresponding to the systems in Fig. 5 are shown for a small binding energy in Fig. 6. We see again that the large tail of the neutral system is reduced as the Coulomb potential is increased. Although the two-proton tail still has not disappeared altogether, it is clear that an additional Coulomb potential, obtained by increase of either core or halo charge, will confine the system to “normal” sizes.

#### IV. APPLICATION IN PRACTICE

Except at the drip lines the threshold for separation of two nucleons will lie above the threshold for separation of one nucleon. Examples of three-body halos are therefore most likely to be found at the drip lines, since the region of high excitation energy where they would appear closer to stability is harder to investigate experimentally. We apply in this section the general theory developed above to some specific nuclei. A better description of these nuclei can of course be obtained with more detailed and dedicated studies as has already been done [9], e.g., for  ${}^6\text{He}$  and  ${}^{11}\text{Li}$ . However, here we are mainly interested in extracting the general features and therefore do not need such a level of sophistication.

##### A. When halos appear

To apply the scaling in Fig. 2 between size and energy for a given nucleus one must obtain a value for  $\rho_0$ , which

obviously is related to the potential between core and halo particles. This potential in turn is related to the density distribution of the core nucleus. As the potential has a larger radius than the density, we may write

$$\langle r^2 \rangle_{\text{pot}} = \langle r^2 \rangle_{\text{core}} + \Delta^2, \quad (19)$$

where  $\Delta$  then has to be estimated. If the potential is found by folding the point density and the nucleon-nucleon interaction used in Sec. III we obtain  $\Delta = 2.20$  fm for Gaussian and 2.05 fm for square well potentials. Using the measured point radius of the core and a given form of our potential,  $\rho_0$  is computed from the appropriate relation in Sec. III A. The value of  $\langle \rho^2 \rangle$  is then found from Fig. 2 and the total rms radius for a system with core mass number  $A_c$  and total mass number  $A = A_c + 2$  is given by

$$\langle r^2 \rangle_{\text{tot}} = \frac{A_c}{A} \langle r^2 \rangle_{\text{core}} + \frac{1}{A} \langle \rho^2 \rangle. \quad (20)$$

For a given energy the rms radii are more sensitive to the value for the potential range than was the case [4] for two-body systems. For  $s$  waves one there had an asymptotic scaling law

$$\frac{\langle r^2 \rangle}{R_0^2} \propto \frac{1}{ER_0^2}, \quad (21)$$

where  $R_0$  was the radius of the potential well. The rms radius is therefore independent of  $R_0$  in the limit of vanishing binding energy. For the three-body case we have instead from the behavior displayed in Fig. 2, which in turn was derived from Eq. (11), that

$$\langle \rho^2 \rangle \propto \begin{cases} \rho_0^2 \ln(\kappa\rho_0), & K = 0, \\ \rho_0^2 \times \text{const}, & K \neq 0, \end{cases} \quad (22)$$

where the larger sensitivity to  $\rho_0$  is seen explicitly. The scaling with the square of the core radius is the typical behavior for normal nuclei.

The definition of a halo state is not as clear-cut in the three-body case as in the two-body case. Should one use the probability for all particles to be separated from each other or the probability that just a pair is far apart? In terms of  $\rho$  it is clear from Figs. 3, 4 and 6 that the systems generally have a large probability (more than 80%) of being at distances larger than  $\rho_0$ . They reside in the “pocket” created by the combined effect of the repulsive centrifugal barrier and the tail of the effective  $W$  potential. The probability of being in the asymptotic region ( $\rho > \rho_L$ ) will never get close to one, again due to the influence of the centrifugal barrier that here confines the system. If we instead use the probability for one nucleon to be outside the core (independent of the position of the other) as the measure, we find similarly that the probability for having  $r_{cn}$  larger than  $\langle r_{cn}^2 \rangle_{\text{core}}^{1/2}$  (i.e., that the nucleon is outside the bulk of the core) again will be large. On the other hand the probability of being outside the two-body potential ( $r_{cn} > R_{cn}$ ) is more moderate — reaching 90 and 40% asymptotically for small energies for  $K = 0$  and 2, respectively. The probability reaches 50% for  $\langle \rho^2 \rangle / \rho_0^2$  about 3–5. Due to the scaling properties,

a certain probability for being outside the core converts to a fixed ratio of halo to core radii.

A crude estimate indicating when halos appear can be inferred from the mean square radii of two nucleons around a core. It seems reasonable to demand that the ratio  $\langle r_{cn}^2 \rangle / R_{cn}^2$  at least should exceed 1-2 if the state should be considered a halo. For a heavy core  $\langle r_{cn}^2 \rangle \approx \langle \rho^2 \rangle / 2$  and by use of Eq. (17) one finds that the ratio  $\langle \rho^2 \rangle / \rho_0^2$  should be at least 3-6. (This incidentally agrees with the alternative definition  $\langle \rho^2 \rangle \geq \rho_L^2$ , since  $\rho_L$  can be expected to be a few times larger than  $\rho_0$ .) Referring back to Fig. 2 we would therefore consider  $K = 0$  and  $K = 1$  states at low binding energy as halo states, whereas more detailed calculations are needed to decide for a  $K = 2$  state.

As already shown the two-body systems are more divergent in the limit of small binding energy, but it is noteworthy that the mean square radii are quite similar at binding energies of a few hundred keV. For very small binding energies we certainly expect the two-body systems to give larger effects, but for "normal halos" at binding energies 100 keV or larger, we would expect two- and three-body systems to give experimental signatures of similar magnitude. When one goes to heavier systems  $R_{cn}$ , and as seen from Sec. III A therefore also  $\rho_0$  will scale as  $A^{1/3}$ . It follows immediately from Eqs. (20)-(22) that all our conclusions drawn for light nuclei can be transferred provided the binding energies are scaled as  $A^{-2/3}$ . As a general rule we therefore conclude that halos only can appear for states with  $EA^{2/3}$  less than a few MeV.

### B. Halo states

We list in Table I some nuclear states that should be well described as consisting of three particles. It gives

some basic experimental quantities and our calculated value for the halo size and for the probability  $P_{out}$  of having  $r_{cn} > R_{cn}$ . An explicit calculation was done for each case with a square well potential, the radius of which is also listed.

Among the nuclei mentioned in Table I the ground state of  ${}^6\text{He}$  and its isobaric analog state, the lowest isospin 1 state in  ${}^6\text{Li}$ , are unique since the nucleon-core potential is well known. Detailed *ab initio* calculations can therefore be performed [9]. These nuclei are special in the sense that the core (an alpha particle) is tightly bound and small and the computation therefore sensitive to the average value chosen for  $\Delta$ . The total rms radius for  ${}^6\text{He}$  would from our calculations be 2.36 fm, which can be compared with the experimental value [24] of  $2.52 \pm 0.03$  fm.

Much work has also been done on the nucleus  ${}^{11}\text{Li}$ , see, e.g., the review in [9]. Here, as in the other cases in Table I, the core is unstable and the nucleon-core potential is consequently not very well known. It is not even known with certainty in what orbitals the two outer neutrons are placed; we have therefore calculated both for the cases  $K = 0$  and  $K = 2$ . The resulting total rms radii become 3.37 fm and 2.79 fm, respectively, to be compared with the value of  $3.10 \pm 0.17$  fm extracted from experiment. For  $K = 0$  the sensitivity of the rms radius to variations in the energy is about 1.5 fm/MeV at  $-E = 0.25$  MeV. Even though the latter value does not include the uncertainty stemming from the extraction procedure (see Ref. [24]) these values still indicate that the  $K = 0$  and  $K = 2$  components in  ${}^{11}\text{Li}$  are comparable. Note also that the cross section for processes as  ${}^{11}\text{B}(\pi^-, \pi^+){}^{11}\text{Li}$  will converge to a constant as the binding energy vanishes even for a pure  $K = 0$  solution. This deviates drastically from the  $r_{2n}^{-6}$  scaling ( $r_{2n}$  is the rms

TABLE I. Halo states in the one hyperharmonic approximation. For each state the binding energy, the rms core radius with corresponding potential radius and the  $K$  quantum number of the halo particles are listed. The probability  $P_{out}$  for a neutron to be outside the neutron-core potential and the expectation values of  $\rho^2$  for the halo particle and the total rms radius of the system calculated for a square well potential is given in the last columns.

Nucleus	$-E^a$ (keV)	Configu- ration	$\langle r_{core}^2 \rangle^{1/2 b}$ (fm)	$R_{cn}$ (fm)	$K$	$P_{out}$ (%)	$\langle \rho^2 \rangle$ (fm <sup>2</sup> )	$\langle r_{tot}^2 \rangle^{1/2}$ (fm)
${}^6\text{He}$	975	$n + n + {}^4\text{He}$	1.59	3.35	2	49	23.3	2.36
${}^{11}\text{Li}$	250 <sup>c</sup>	$n + n + {}^9\text{Li}$	2.32	4.00	0	60	76.2	3.37
					2	47	37.1	2.79
${}^{14}\text{Be}$	1120	$n + n + {}^{12}\text{Be}$	2.58	4.25	0	42	42.8	2.96
					2	41	36.2	2.88
${}^{17}\text{B}$	1520 <sup>c</sup>	$n + n + {}^{15}\text{B}$	2.40	4.07	0	39	36.3	2.69
					2	40	32.9	2.65
${}^{19}\text{B}$	500	$n + n + {}^{17}\text{B}$	2.65 <sup>d</sup>	4.33	0	52	63.0	3.10
					2	44	41.5	2.91
${}^6\text{Li}^e$	136	$n + p + {}^4\text{He}$	1.59	3.35	2	50	24.5	2.40
${}^{17}\text{Ne}$	950	$p + p + {}^{15}\text{O}$	2.72 <sup>f</sup>	4.40	0	20	23.6	2.81

<sup>a</sup>From Ref. [23] except where noted.

<sup>b</sup>From the point density. From Ref. [24] except where noted.

<sup>c</sup>Reference [25].

<sup>d</sup>Our calculated value.

<sup>e</sup>The excited state at 3.56 MeV, all other states are ground states.

<sup>f</sup>The  ${}^{16}\text{O}$  radius charge.

radius of the last two neutrons) suggested in [26].

The nuclei  $^{14}\text{Be}$  and  $^{17}\text{B}$  are not nearly as loosely bound so that the difference between the total rms radius for  $K = 0$  and  $K = 2$  becomes quite small. None of them can be considered as having well-developed halos. The experimental value of the rms radius of  $^{14}\text{Be}$  is  $3.1 \pm 0.4$  fm, which is consistent with our calculated value of 2.9 fm.

There is very little experimental information available on the nucleus  $^{19}\text{B}$ , but mass extrapolations predict it to be rather loosely bound. We have used a binding energy for the last two neutrons of 500 keV and our calculated core radius for  $^{17}\text{B}$  to estimate its radius. If the binding energy does turn out to be low,  $^{19}\text{B}$  could become as interesting as  $^{11}\text{Li}$ . There are more potential ground-state two-neutron halo nuclei further up the neutron drip-line, e.g.,  $^{22}\text{C}$  and  $^{29}\text{F}$ , but their binding energies are again not yet experimentally known and one can only hope that some of them will turn out to be very loosely bound and therefore interesting.

The first Borromean nucleus on the proton drip line is  $^{17}\text{Ne}$  (if one excepts  $^{10}\text{C}$  for which both the one- and two-proton daughters,  $^9\text{B}$  and  $^8\text{Be}$ , are unbound — it has a two-proton separation energy of 3.8 MeV), but as seen from the calculated radius it can hardly be counted as a halo even if  $K$  should turn out to be zero. The Coulomb confinement effects are too large for this case of two protons outside 8 unit charges in the core.

## V. SUMMARY AND CONCLUSIONS

We have investigated the asymptotic behavior of the nuclear three-body problem for small binding energies. The system interacts through two-body potentials, which are so weak that no binary subsystem is bound, although the three particles are bound in a quantum mechanical state. The interactions are of short range except for charged systems where the Coulomb potential enters. We speak of a core and two halo particles although this terminology sometimes is rather artificial. The basic assumption is that all three “particles” are inert and the corresponding intrinsic degrees of freedom are completely decoupled. Thus the results are only applicable when the particle overlaps turn out to be small.

We use the hyperharmonic expansion and assume for simplicity that all “particles” are spinless. The method is simple and useful for these systems, where usually about 90% of the wave function is in a state of given so-called hyperharmonic quantum number  $K$ . An accurate calculation of the binding energy for a given set of interactions requires that many  $K$  values are included in the expansion. However, the functions with different  $K$ -values decouple at large distances for short-range potentials and we are left with an effective radial equation with a centrifugal barrier term and a potential falling off at least as the third power of the distance.

For each  $K$  we compute analytically for short-range potentials the asymptotic behavior of the radial moments in the low binding energy limit. The results are easily obtained from corresponding two-body systems by the

substitution  $l = K + 3/2$  where  $l$  is the two-body angular momentum. The second radial moments are all convergent for vanishing binding energy except that of  $K = 0$ , which diverges logarithmically. In general, the lower the  $K$ , the faster the divergence, the higher the  $K$ , the smaller the system. A mixture of  $K$  values therefore, in the extreme low-energy region, lead to a size of the system which is determined by the lowest possible value of  $K$ . When this  $K$  value is also the dominating component in the wave function, the asymptotic behavior is determined accordingly. When a higher  $K$  value dominates the wave function, it also determines the asymptotic behavior of the radial moment for all binding energies of interest in the nuclear context.

An approximate scaling of size versus energy is found independent of the details of the potential even when the asymptotic mean square radius is finite. This results in a universal scaling plot (Fig. 2) of the second radial moment versus binding energy. We argued that halos would appear for  $\langle \rho^2 \rangle / \rho_0^2$  above 5, i.e., mainly for  $K = 0$  and 1. The asymptotic behavior is reached at about 0.2 MeV for light nuclei and at smaller energies for heavier nuclei. This implies that halos only can be expected to show up for heavier nuclei at binding energies scaled down by the square of the characteristic length. Crudely speaking the limiting binding energy should then behave like  $1 \text{ MeV}/A^{2/3}$ . In this connection it is worth emphasizing that halo states may be ground states as well as excited states.

Inclusion of repulsive power law ( $1/\rho^\nu$ ) potentials, like the Coulomb interaction for charged particles, confine (for  $0 < \nu < 2$ ) all radial moments to finite values for all binding energies. The asymptotic wave function  $[(\lambda\rho)^{1/4} \exp(-2\sqrt{\lambda\rho})$  for a Coulomb potential with an inverse effective Coulomb length parameter  $\lambda$ ] for zero energy decreases fast enough to make all radial moments finite. The confinement due to the Coulomb interaction is rather severe and already two protons outside a core charge of three units limit the extension significantly compared to the case of two neutrons outside a core.

Only a few three-body halos have been investigated experimentally. Table I gives our numerical results for these cases and for a few heavier nuclei.

A three-body system certainly gives room for more types of structures than a two-body system. Rather general results could however be obtained here for the weakly bound nuclear three-body systems where no binary subsystems are bound. Even though the extreme asymptotic limits might not be realized in nature our results are useful not only as a “guideline” or “reference unit” but also, due to the scaling, for qualitative first estimates of the two-nucleon halo nuclei on the drip lines.

## ACKNOWLEDGMENTS

We are grateful to M. V. Zhukov for his encouragement and helpful advice. We also want to thank I. Thompson and B. V. Danilin for discussions concerning the numerical calculations. One of us (D.V.F.) acknowledges support from the Danish Research Council.

### APPENDIX A: HYPERSPHERICAL HARMONICS

We consider a system of three particles with masses  $m_i$  and coordinates  $\mathbf{r}_i$ . The Jacobi coordinates, see Fig. 1, are defined as

$$\begin{aligned} \mathbf{x}_i &= a_{jk} \mathbf{r}_{jk}, \quad \mathbf{y}_i = a_{(jk)i} \mathbf{r}_{(jk)i}, \\ a_{jk} &= \left( \frac{1}{m} \frac{m_j m_k}{m_j + m_k} \right)^{1/2}, \end{aligned} \quad (\text{A1})$$

$$\begin{aligned} a_{(jk)i} &= \left( \frac{1}{m} \frac{(m_j + m_k) m_i}{m_1 + m_2 + m_3} \right)^{1/2}, \\ \mathbf{r}_{jk} &= \mathbf{r}_j - \mathbf{r}_k, \quad \mathbf{r}_{(jk)i} = \frac{m_j \mathbf{r}_j + m_k \mathbf{r}_k}{m_j + m_k} - \mathbf{r}_i, \end{aligned}$$

where  $i, j, k$  is a cyclic permutation of 1, 2, 3, and  $a^2$  are the reduced masses of the subsystems in units of  $m$ , which is a normalization mass chosen to be equal to the nucleon mass.

The hyperspherical variables [16] are introduced as

$$\rho, \quad \mathbf{n}_{x_i} = \mathbf{x}_i / |\mathbf{x}_i|, \quad \mathbf{n}_{y_i} = \mathbf{y}_i / |\mathbf{y}_i|, \quad \alpha_i, \quad (\text{A2})$$

where  $\alpha$  is in the interval  $[0, \pi/2]$

$$\rho^2 = \mathbf{x}_i^2 + \mathbf{y}_i^2, \quad |\mathbf{x}_i| = \rho \cos \alpha_i, \quad |\mathbf{y}_i| = \rho \sin \alpha_i. \quad (\text{A3})$$

We omit the indices where we need not emphasize the particular set of Jacobi coordinates. Note that  $\rho$  is independent of what set is used. The kinetic energy operator is in these coordinates

$$T = -\frac{\hbar^2}{2m} \left[ \frac{d^2}{d\rho^2} + \frac{5}{\rho} \frac{d}{d\rho} - \frac{\hat{K}^2(\Omega)}{\rho^2} \right], \quad (\text{A4})$$

where  $\hat{K}^2(\Omega)$  is an angular operator. It has the eigenvalues  $K(K+4)$  and the hyperspherical harmonics  $(\mathbf{Y}_K)$  as eigenfunctions

$$\begin{aligned} \mathbf{Y}_K &= N_K (\cos \alpha)^{l_x} (\sin \alpha)^{l_y} P_n^{l_y+1/2, l_x+1/2}(\cos 2\alpha) \\ &\quad \times [Y_{l_x}(\mathbf{n}_x) Y_{l_y}(\mathbf{n}_y)]_{LM}, \\ K &= (K, l_x, l_y, L, M), \quad n = (K - l_x - l_y)/2, \\ N_K &= \left( \frac{n!(n+l_x+l_y+1)! 2(K+2)}{\Gamma(n+l_x+3/2)\Gamma(n+l_y+3/2)} \right)^{1/2}, \end{aligned} \quad (\text{A5})$$

where  $Y_{l_x}, Y_{l_y}$  are ordinary spherical harmonics,  $P_n^{\alpha, \beta}$  is the Jacobi polynomial of order  $n$  ( $n$  must be a non-negative integer), and  $\Gamma$  is the gamma function. The total angular momentum  $L$  and its projection  $M$  is obtained by coupling the relative angular momenta,  $l_x$  and  $l_y$ , corresponding to the  $x$  and  $y$  coordinates. Only the total angular momentum  $L$  is a conserved quantity which may be obtained by coupling of different combinations of  $l_x$  and  $l_y$ .

Extracting the factor  $\rho^{-5/2}$  from the radial wave function allows one to get rid of the first derivative in the radial equation and leads to the  $(K+3/2)(K+5/2)/\rho^2$  form of the centrifugal barrier.

The quantum number  $K$  corresponds to definite combinations of relative two-body states. As an example consider the case of two nucleons around a heavy core and let  $\mathbf{x}$  be the nucleon-nucleon distance. Then a state with  $(K, L, l_x, l_y) = (0, 0, 0, 0)$  will correspond to the two nucleons being in  $s$  waves relative to the core. A state with  $(K, L, l_x, l_y) = (2, 0, 0, 0)$  corresponds to the two nucleons being mainly in  $p$  waves (already 99% for a core of mass 9). Finally,  $(K, L, l_x, l_y) = (1, 0, 0, 1)$  corresponds mainly to one nucleon in a  $p$  wave and the other in an  $s$  wave.

- 
- [1] P.G. Hansen and B. Jonson, *Europhys. Lett.* **4**, 409 (1987).
  - [2] P.G. Hansen, *Proceedings of the International Nuclear Physics Conference, Wiesbaden, 1992* [*Nucl. Phys.* **A553**, 89c (1993)].
  - [3] I. Tanihata, *Nucl. Phys.* **A522**, 275c (1991).
  - [4] K. Riisager, A.S. Jensen, and P. Møller, *Nucl. Phys.* **A548**, 393 (1992).
  - [5] D.V. Fedorov, A.S. Jensen, and K. Riisager, *Phys. Lett. B* **312**, 1 (1993).
  - [6] V. Efimov, *Phys. Lett.* **33B**, 563 (1970); *Comments Nucl. Part. Phys.* **19**, 271 (1990).
  - [7] Y. Tosaka, Y. Suzuki, and K. Ikeda, *Prog. Theor. Phys.* **83**, 1140 (1990).
  - [8] A.S. Jensen and K. Riisager, *Phys. Lett. B* **264**, 238 (1991); *Nucl. Phys.* **A537**, 45 (1992).
  - [9] M.V. Zhukov, B.V. Danilin, D.V. Fedorov, J.M. Bang, I.S. Thompson, and J.S. Vaagen, *Phys. Rep.* **231**, 151 (1993).
  - [10] L. Johannsen, A.S. Jensen, and P.G. Hansen, *Phys. Lett. B* **244**, 357 (1990).
  - [11] Y. Tosaka and Y. Suzuki, *Nucl. Phys.* **A512**, 46 (1990).
  - [12] G.F. Bertsch and H. Esbensen, *Ann. Phys.* **209**, 327 (1991).
  - [13] T. Otsuka, N. Fukunishi, and H. Sagawa, *Phys. Rev. Lett.* **70**, 1385 (1993).
  - [14] N.Ya. Vilenkin, *Special Functions and the Theory of Group Representations* (American Mathematical Society, R.I., 1968), Chap. 10.
  - [15] J. Raynal and J. Revai, *Nuovo Cimento A* **68**, 612 (1970).
  - [16] R.I. Jibuti and N.B. Krupennikova, *The Hyperspherical Functions Method in Few-Body Quantum Mechanics* (Mecniereba, Tbilisi, 1984).
  - [17] S.P. Merkuriev, *Yad. Fiz.* **19**, 447 (1974) [*Sov. J. Nucl. Phys.* **19**, 222 (1974)].
  - [18] B.V. Danilin, M.V. Zhukov, A.A. Korsheninikov, L.V. Chulkov, and V.D. Efros, *Yad. Fiz.* **49**, 351 (1989) [*Sov. J. Nucl. Phys.* **49**, 217 (1989)].
  - [19] M.V. Zhukov, B.V. Danilin, D.V. Fedorov, J.S. Vaagen, F.A. Gareev, and J.M. Bang, *Phys. Lett. B* **265**, 19

- (1991).
- [20] A.M. Badalyan and Yu.A. Smirnov, *Yad. Fiz.* **3**, 1032 (1966) [*Sov. J. Nucl. Phys.* **3**, 755 (1966)].
- [21] G.E. Brown and A.D. Jackson, *The Nucleon-Nucleon Interaction* (North-Holland, Amsterdam, 1976).
- [22] D. Gogny, P. Pires, and R. de Toureil, *Phys. Lett.* **32B**, 591 (1970).
- [23] A.H. Wapstra, G. Audi, and R. Hoekstra, *At. Data Nucl. Data Tables* **39**, 281 (1988).
- [24] I. Tanihata, T. Kobayashi, O. Yamakawa, S. Shimoura, K. Ekuni, K. Sugimoto, N. Takahashi, T. Shimoda, and H. Sato, *Phys. Lett. B* **206**, 592 (1988).
- [25] J. Wouters, R.H. Kraus, Jr., D.J. Vieira, G.W. Butler, and K.E.G. Löbner, *Z. Phys. A* **331**, 229 (1988).
- [26] W.R. Gibbs and A.C. Hayes, *Phys. Rev. Lett.* **67**, 1395 (1991).